m^{6}A-related lncRNA-based immune infiltration characteristics and prognostic model in colonic adenocarcinoma

Hao-lun Wang
Guangxi Medical University
zhuo-miao Ye
Xiangya Hospital Central South University
Zi-yun He
Guangxi Medical University
Lu Huang
Guangxi Medical University
Zhi-hui Liu (lzhh101@sina.com)
Guangxi Medical University First Affiliated Hospital: The First Affiliated Hospital of Guangxi Medical University

Research

Keywords: immune infiltration, prognostic model, m6A-related lncRNA, colonic adenocarcinoma

Posted Date: May 24th, 2022

DOI: https://doi.org/10.21203/rs.3.rs-1616846/v1

Version of Record: A version of this preprint was published at Hereditas on February 9th, 2023. See the published version at https://doi.org/10.1186/s41065-023-00267-y.

Abstract

Background: Colonic adenocarcinoma (COAD) is a common gastrointestinal tract tumor, and its occurrence and progression are usually associated with genomic instability, tumor suppressor gene and oncogene mutations, and tumor mutational load.The biological importance of RNA N6-methyladenosine (m6A) modification and long non-coding RNA (lncRNA) expression in tumorigenesis and progression has been demonstrated. However, the regulatory role of m6A - associated lncRNAs in the tumor microenvironment (TME) and the stratification of prognosis and immunotherapy have not been determined.

Methods: We screened 43 prognostic lncRNAs linked to m6A and conducted consistent molecular typing of COAD using consensus clustering. The ssGSEA algorithm and the ESTIMATE algorithm were employed to assess the immune characteristics describing the different subgroups. Covariation between methylation-related prognostic lncRNAs was then eliminated by least absolute shrinkage and selection operator (Lasso) Cox regression. A nomogram was created and evaluated by combining the methylation-related prognostic lncRNA model with other clinical factors. And, the relationship between prognostic model grouping and microsatellite instability (MSI), immunophenotype score (IPS) and tumor mutation burden (TMB) was further validated using R language. Finally we used the linkage map (CMAP) to filter sensitive medicines to suppress the expression of high-risk genes.

Results: Three separate m6A-associated lncRNA modes were discovered in 446 COAD specimens with different clinical endpoints and biological status. Risk scores were constructed based on m^6A-associated lncRNA signature genes. Patients with lesser risk scores demonstrated superior immunotherapy response and clinical benefit. Further profiling suggested that lesser risk scores were also correlated with higher IPS scores, tumor mutation burden, and mutation rates in significant mutated genes (SMGs) (e.g., FAT4 and MUC16). Piperidolate, quinostatin, and mecamylamin were then screened for their ability to suppress expression of high-risk genes in the model.

Conclusions: Quantitative assessment of m6A-associated lncRNAs in single tumors is expected to enhance our comprehension of the TME profile. M6A-associated lncRNAs constructed a prognostic model that facilitates prognosis and immunotherapy stratification in COAD patients, and based on the model we screened three drugs with potential therapeutic value.

1. Background

Adenocarcinoma of the colon (COAD) is a common gastrointestinal tumor which incidence and mortality rates are the highest in the third and fourth, respectively [1, 2]. There are more than 1 million newly diagnosed COAD patients each year, of which about 600,000-700,000 patients die from COAD[2, 3].

Colorectal cancer (CRC) is a general term for malignant tumors of colon epithelial origin. Colonic adenocarcinoma (COAD) is the most common histological type of all colon cancers. Its occurrence and development are usually related to genomic instability, tumor suppressor gene and oncogene mutation

and expression disorder, tumor mutation burden, and other factors. CRC is not only highly heterogeneous at the genetic level, but also highly heterogeneous at the molecular level [4]. This has a great influence on the prognosis of patients, the effectiveness of the available immunotherapy, and a clear understanding of the principles of molecular of CRC development and progress to promote the diagnosis and treatment is important in the future.

TME refers to the tumor or cancer stem cells reside environment and contains cells and molecules, increase the tumor cell is dry, promote angiogenesis, mediation of migration, reduce drug sensitivity, inhibit the autoimmune defense system. Better understanding of TME, its function and related molecular biology provide important insights into the different tumors, and the key targets of new cancer therapies are cancer-promoting processes and molecules in TME [5].

As a new type of cancer treatment, immunotherapy stimulates and boosts the immune system's ability to fight cancer cells, especially the *PD-1*/*PD-L1*, which is effective in CRC and is considered one of the most promising approaches for treating CRC. In patients with CRC characterized by DMMR or microsatellite instability (MSI) mutations, tumors are usually characterized by high mutation burden, abundant tumor-infiltrating lymphocytes (TILS), and upregulated PD-L1 expression in the tumor microenvironment. It can also lead to a better prognosis after treatment in patients with PD − 1 / PD - L1 [6],[7].

RNA methylation modification m^6A, this is methyl adenosine N6 position, is a broad and abundant changes in messenger RNA (mRNA) and noncoding RNA (ncRNA), dynamic regulating of the genesis and development of tumors [8]. m^6A is dynamically adjusted by special methyltransferases (Writers) and demethylases (Erasers). Mutations and disorders in the specific methyltransferas and demotylas often relate to the occurrce, progrsion, metastasis, and tumor recurrce [9].

The m^6A methylation also often occurs in the poly(a) region of lncRNAs. The imbalance of m^6A modification may lead to abnormal expression of lncRNAs, and lncRNAs can regulate gene expression through transcriptional and histone modifications, increase chromosomal instability and participate in cancer cell growth, metastasis, and drug resistance[9],[10] as a way to regulate tumor progression. Screening for prognostic lncRNAs associated with m^6A can be used as an important indicator to evaluate tumor prognosis[11].

m^6A modifications play an integral role in inflammation, innate immunity, and antitumor effects. Although there have been some relevant studies on one or two m^6A regulators[9, 12, 13], the role of lncRNA in TME regulation of COAD still cannot be ignored. In addition, highly heterogeneous COAD occurrence and progression are associated with MSI, MMR, TMB, and other biomarkers. Therefore, it is not possible to assess a particular m^6A-regulated lncRNA alone and there is a need to find new biomarkers to assess along with immune checkpoints and other relevant metrics to gain a comprehensive understanding of various m^6A-related lncRNA-mediated TME profiles and improve prognosis and immunotherapy stratification. Our study was to synthesize genomic information from 514 colorectal cancer samples to comprehensively assess the modification patterns of m^6A-associated

lncRNAs and correlate m^{6}A-associated lncRNAs with the infiltration characteristics of TME cells, aiming to systematically assess the m^{6}A-associated lncRNAs with COAD prognosis, immune checkpoints, tumor immune infiltration, and TMB, MSI, and immune scoring association. M6a-related lncRNAs related risk models were established to stratify the prognosis of COAD patients and facilitate treatment decisions,this study also provides a possible regulatory mechanism between tumor microenvironment and M6A, thus providing strategies for immunotherapy of COAD.

2. Materials And Methods

2.1 Datasets

RNA-seq (FPKM format) transcriptome data were downloaded from the public database The Cancer Genome Atlas (TCGA) data portal (https://portal.gdc.cancer.gov/).

On March 31, 2021, data from 473 COAD specimens and 41 adjoining normal tissues were downloaded. And data without clear TNM staging as well as survival information were excluded. Finally, 446 patients with COAD with appropriate clinicopathological details were included in the follow-up analysis.

The Masked Somatic Mutation data (varscan. Somatic. Maf) files for the nucleic acid-only variant samples were similarly obtained from the TCGA data portal. Immune epistasis scores (IPS) and microsatellite instability scores were obtained from the Cancer Immunome Atlas download (https://tcia.at/home).

2.2 Bioinformatics Analysis

We annotated the COAD transcript data obtained by TCGA and divided them into two sections: mRNA expression profile and lncRNA expression profile. Based on the published literature [14–17], we collected and identified 24 m6A RNA methylation regulators from the mRNA expression profile of COAD.

To screen out the lncRNAs associated with m^{6}A RNA methylation regulators, we test the correlation of m^{6}A-related lncRNAs in each dataset with Pearson correlation analysis (|Pearson R|>0.4, $p < 0.001$). As a result, 1612 m^{6}A-related lncRNAs were identified.

Then, we screened a total of 43 m^{6}A-associated prognostic lncRNAs in TCGA data by one-way Cox regression analysis. Furthermore, we determined the differential expression of 43 m^{6}A-associated prognostic lncRNAs in tumor tissues and adjacent normal tissues.

We classified patients with COAD into different subtypes using the "ConsensusClusterPlus" R package. And then principal component analysis (PCA) was performed to verify gene expression patterns between different COAD isoforms, and scatter plots were plotted using the R package "ggplot2".

We performed GSVA analysis using the R package 'GSVA' to investigate the differences in biological processes between different m^{6}A modification patterns. Explicit biological features were derived from the

Hallmark gene set [18] (downloaded from MSigDB database v7.1) and Mariathasan et al. constructed gene sets[16] (selected from the IMLIGN210CoreBiology package).

Estimation of stromal and immune cells in malignant tumors was performed using an expression data (ESTIMATE) algorithm [19], which uses the unique properties of transcriptional profiles to infer tumor cell density and tumor purity. By using the R " estimate " package to perform the algorithm, we calculated immune and mesenchymal scores to predict the level of infiltrating immune and stromal cells.

Immunoepitope score (IPS) is a better predictor of response to anti-CTLA-4 and anti-PD-1 options [20]. We determined the differences in their CTLA-4 and anti-PD-1 options by comparing IPS in different clusters and high- and low-risk cohorts.

Relative abounds of 23 immune cell types in the tumor microenvironment were measured using single-sample gene set enrichment analysis (ssGSEA) as a way to compare different levels of immune infiltration between clustered subtypes and risk score subgroups.

The least absolute shrinkage and selection operator (LASSO) was used to construct the best risk model for methylation-associated lncRNAs. Risk scores were then calculated for each patient based on the model. Patients with COAD cancer were classified into high- and low-risk groups by the median of the risk scores.

In addition to this, Perl scripts were used to calculate mutation frequency and variant/exon length (38 million) for each sample as a way to compared differences in tumor mutation load between clustered subtypes and risk score groupings. [21]And the "maftools" [22] R package was used to visualize the mutation types.

Differential analysis was performed by limma R package for high and low risk groups, and then risk differentially expressed genes were screened by adjusting for P-values less than 0.05 and logFC absolute values greater than 1. Finally, the differentially expressed genes were uploaded to association mapping (https://portals.broadinstitute.org/cmap/) to screen for sensitive drugs that could inhibit the expression of risk genes in the prognostic model.

2.3 Statistical Analysis

We performed statistical tests with version R4.0.3. The lncRNAs correlated with m6A regulators were screened using pearson correlation analysis and the correlation of risk scores with the level of immune cell infiltration was examined.

Kruskal-Wallis, Wilcoxon rank-sum test was used for intergroup comparison between two subgroups and more than two subgroups.

Cox regression models were performed for both univariate and multifactorial analyses to identify the independent prognostic value of clinical characteristics and prognostic predictors. According to the findings of multivariate Cox proportional risk analysis, we made nomogram with the R package "rms"

with the aim of predicting total mortality at 1, 3, and 5 years. The individual patient's prognostic risk can be measured by the score relative to each risk element.

AUC was used to evaluate the predictive effectiveness of m6A-related lncRNAs model and Nomogram survival prediction model for OS at 1, 3 and 5 years.

Categorical variables were used to compare the training and validation groups using chi-square tests. In the SMG analysis, fisher's exact test was used to examine statistical differences in gene mutations between the high-risk and low-risk groups.

The Kaplan-Meier method was used for the survival curves, and the log-rank test was used for comparison between groups.

3. Result

3.1There are 43 m^6A regulator-associated prognostic lncRNAs in COAD

First, to explore m^6A regulator-associated lncRNAs, the expression matrices of 43 m6A regulators in TCGA database are extracted and identified 14086 lncRNAs for subsequent analysis. Then, we searched for m^6A-associated lncRNAs in each dataset by Pearson correlation analysis. If lncRNAs are related to m6A, their expression value should be related to at least one of the 24 regulatory factors of m6A ($|Pearson\ R|>0.4$, $p < 0.001$). Our results showed 1612 lncrnas significantly related with M6A. The LncRNAs significantly correlated with related genes were combined with prognostic information, and the lncrnas associated with M6A were selected by univariate Cox regression ($P < 0.03$). Finally, we found that 43 lncRNAs which related to m^6A from the TCGA database were significantly associated with OS in COAD patients, of which all were negatively associated with OS except *AL137782.1*, *AC073896.3* and *AC104819.3* (Fig. 1B). Further observation of the 43 m^6A-related prognostic lncRNAs with m^6A regulators revealed that all of them were positively correlated except RBM15B and ALKBH5 were the negatively relationship with M6A-related prognostic lncrnA, the rest were statistically significant positive correlated (Fig. 1A).

3.2 The expression characteristics of lncRNA and immune checkpoint related to m6A methylation in COAD

To evaluate the biological function of lncRNAs associated with m6A methylation in the progression of COAD, Based on the existing Cancer Genome Map (TCGA) data, we systematically studied the expression of 43 m6A methylation-related prognostic lncRNAs in COAD and its adjacent normal tissues. We obtained data sets of expression profiles from 473 tumor tissues and 41 paracancer normal tissues and performed differential expression analysis of selected m^6A regulator-associated prognostic lncRNAs. m^6A methylation-associated prognostic lncRNAs were significantly different in expression levels in COAD and normal tissues, showing an overall upregulation of expression (Fig. 1C and 1D).

Except for *SNHG26*, *AC145285.2*, *AC026367.1* (P < 0.05), *AC092944.1*, *GLIDR*, *AL512306.3*, *U91328.1*, *ATP2B1-AS1*, *PRKAR1B-AS2*, *SEPTIN7-DT*, *AC104819.3*, *NIFK-AS1*, *AC019205.1*, *LINC01588*, *LINC00861* (P < 0.001) were abundant in normal tissues adjacent the cancer, and the rest were abundant in COAD tissues.Our results suggest that m^6A methylation-associated prognostic lncRNAs have an significant biological role in the progression of COAD. By comparing 8 common immune checkpoints in COAD tumor and paracancer tissues, we found that their expression was inconsistent. the expression levels of *PDCD1LG2* (P < 0.01), *LAG3* (P < 0.001) were higher in normal paracancer tissues, while *SIGLEC15* with *CTLA4* (P < 0.001) were more expressed in COAD tissues. The rest were not statistically different (Fig. 1E).

3.3 Association of m^6A methylation-related prognostic lncRNAs consensus clustering with COAD patient characteristics and survival

Based on the similarity between the expression level of lncRNA related to m6A regulator and the proportion of fuzzy clustering measure, k = 3 was determined, and the optimal clustering stability was k = 2–9 (Fig. 2A). Then, principal component analysis (PCA) method was used to further analyze the gene expression profile between the two isomers, and it was found that there were good differences among the three isomers. (Fig. 2B). According to the expression level of m6A regulator, 446 patients with COAD were divided into three subtypes : cluster A (n = 234), cluster B (n = 42) and cluster C (n = 170). The prognostic lncRNA related to m6A methylation in group B was generally significantly higher than that in the other two groups, especially in group A. (Fig. 2C).

The clinical attributes of the three subtypes were compared (Fig. 2C). The TNM staging ratio of gene cluster B was higher than that of gene cluster A and C (p < 0.01). Cluster A and C had a lower proportion of patients with distant metastases and lymph node metastases than cluster B (p < 0.05).

The Log-rank p value of Kaplan-Meier curve was 0.004, indicating that the OS difference among lncRNA clusters of three m6A methylation-related prognosis was statistically significant (Fig. 2D). The overall survival rate of group B was significantly lower than that of the other two groups.

3.4Consensus clustering of m^6A methylation-associated prognostic lncRNAs associated with different TMEs

To study the of effect of m6A methylation-related prognostic lncRNA on tumor immune microenvironment in patients with COAD, we assess ed the Immunization scores, stromal scores, and immune cell infiltration levels of m^6A methylation-associated prognostic lncRNAs among the presenting high, low and medium expression of cluster A, cluster B and cluster C, respectively (Fig. 3A, B and C).

To investigate potential molecular regulatory mechanisms underlying the differences in grouping of two different m6A associated prognostic lncrnas, we conducted a GSVA enrichment analysis of the hallmark gene set (Fig. 3E, F, G). By analyzing GSVA, cluster A was significantly enriched in immune activation-associated pathways, including complement response, inflammatory response, and allogeneic transplant

rejection. In addition, it was also enriched in cancer suppressor pathways such as P53 and apoptosis, but also in PI3K/AKT/ mTOR, KRAS, IL2/STAT5, and MTORC1 pathways that contribute to cancer progression. cluster C was similar to A, significant enrichment of pathways related to immune activation and tumor suppressor pathways, as well as pathways related to cancer progression, such as P53 and apoptosis and INFα and IL2/STAT5 pathways, PI3K/AKT/mTOR, IL2/STAT5 signaling, and MTORC1, but less than cluster A. On the contrary, cluster B is present with inhibition of immune pathways and downregulation of pathways associated with cancer inhibition.

Enrichment of Cluster A Subtype Related to Epithelial-mesenchymal Transition and Transforming Growth Factor-β is shown in the bar chart (Fig. 3D). This enrichment suggests a significant enhancement of mesenchymal activation.

3.5 Exploring the clinical significance of consensus clustering of methylation-related prognostic lncRNAs

In order to further study clinical significance of m^6A methylation-related prognostic lncRNAs, we further predicted the difference in immunotherapy between the three clustering subgroups according to the IPS (Fig. 4A, B), with cluster C outperforming cluster A when *CTLA4* was administered alone ($P < 0.05$), while the treatment effect between cluster C and B There was no difference between groups C and B. The treatment effect of cluster C was better than that of cluster B when *CTLA4* and *PD1* were combined ($P < 0.001$), and there was no difference in the treatment effect between Groups C and A. These results suggest that m^6A methylation-related prognostic lncRNA factors may be able to influence the effect of immunotherapy.

The differences of the 8 immune checkpoints between the different cluster subgroups are shown in (Fig. 4C), except for the expression of *CTLA4*, which was not statistically significant among the three subgroups, the expression of all other immune checkpoints were different (*HAVCR2*, *PDCD1LG2*: $P < 0.001$; *CD274*, *PDCD1*, *LAG3*: $P < 0.01$; *TIGIT*, *SIGLEC15*:$P < 0.05$). Eight immune checkpoints had the best expression and highest immune scores in cluster A.

3.6 Construction of a prognostic model of methylation-related lncRNAs and Validation

Next, the prognostic role of m6A methylation related prognosis lncrnas in COD patients was examined. 446 patients were randomly divided into TCGA training cohort (270 cases) and verification cohort (176 cases) according to the ratio of 6 :. There were no statistical differences in baseline characteristics, age, gender, TNM between the TCGA training and testing cohorts (all $p > 0.05$. Table S1).

Accurately predicting clinical outcomes of m^6A methylation-associated prognostic lncRNAs in COAD patients, We performed LASSO analysis for a total of 43 m6A methylation-associated prognostic lncRNAs in the TCGA training cohort. 13 prognostic predictive signatures of m^6A methylation-associated lncRNA were identified, namely *AC092944.1*, *AL137782.1*, *U91328.1*, *AC073896.3*, *ATP2B1-AS1*,

AL391095.2, *SEPTIN7-DT*, *AC104819.3*, *LINC00861*, *AC003101.2*, *AC005229.4*, *AC156455.1*, *AP001628.1*. (Fig. 5A and B). The coefficients obtained by LASSO can be used to calculate the risk scores of the training and validation sets,and the risk score = (1.2907×*AC092944.1* amount of expression) + (-0.3112×*AL137782.1* amount of expression) + (0.1480×*U91328.1* amount of expression) + (-0.2706×*AC073896.3* amount of expression) + (0.7747×*ATP2B1-AS1* amount of expression) + (0.5129×*AL391095.2* amount of expression) + (1.304×*SEPTIN7-DT* amount of expression) + (-0.5918×*AC104819.3* amount of expression) +(0.2377×*LINC00861* amount of expression) +(0.4255×*AC003101.2* amount of expression) +(0.1462×*AC005229.4* amount of expression) + (0.1406×*AC156455.1* amount of expression) +(0.0311×*AP001628.1* amount of expression).

Afterward, We divided the patients into high-risk and low-risk groups according to the median risk score. Figure 5C, D shows the characterization of risk scores, OS status, and expression profiles of the 13 prognostic predictive signatures of m^6A methylation-associated lncRNA in the training and validation cohorts. The heat map revealed that the prognostic predictors in the high-risk group were great higher than those in the low-risk group, except for *AL137782.1*, *AC104819.3*, and *AC073896.3*, whose expression was lower than that in the low-risk group. And *AL137782.1*, *AC104819.3*, *AC073896.3* were also the three m^6A-related prognostic lncRNAs that were positively associated with OS. In the TCGA training and validation cohort, OS was longer in the low-risk group than in the high-risk group ($P < 0.001$ Fig. 5E, F).

In order to evaluate the prediction accuracy of the identified eight risk signals, we analyzed the ROC curve by comparing the area under the AUC values of the training and testing cohorts in 1, 3 and 5 years. In the training cohort, the 1-year, 3-year, and 5-year AUC values for the 13 prognostic factors were 0.787, 0.799, and 0.760, respectively (Fig. 5G) and. In the validation cohort, the 1-year, 3-year and 5-year AUC values for the 13 prognostic signatures were 0.749 and 0.799 and 0.850, respectively (Fig. 5H). The AUC values revealed that the 13 prognostic predictive characteristics of m^6A methylation-associated lncRNA were good discriminators of prognosis in COAD patients. Our findings suggest that the risk score based on 13 prognostic signs can accurately predict the prognosis of patients with COAD.

3.7 The prognostic risk score of COAD correlates with TNM staging and the impact of genetic alterations in predictors on immune cell infiltration

To further evaluate the relationship between risk score and clinical characteristics. The heat map shows the expression levels of 13 prognostic predictors in the high-risk and low-risk groups in the TCGA cohort (Fig. 6A).

Except for *AL137782.1*, *AC104819.3*, and *AC073896.3*, three lncRNAs positively associated with OS, the expression of other 10 predictors was higher in high risk group than in low risk group. High-risk group significantly different compared to low-risk group in the proportions of cluster subtypes ($P < 0.001$) and TNM stage ($P < 0.01$), lymph nodes ($P < 0.05$), and distant metastases ($P < 0.01$).

In addition, the relationship between risk score, cluster subtype and stage, and other clinical features were confirmed. Risk scores were great higher in cluster B than in cluster A ($p < 0.001$) and C ($p < 0.05$, Fig. 6B),

patients with TNM stage III and VI had significantly higher risk scores than patients with stage I and II ($p < 0.001$, Fig. 6C). Risk scores were higher in patients with distant tumor metastases ($p < 0.01$, Fig. 6D) and lymph node metastases ($p < 0.001$, Fig. 6E) than in COAD patients without metastases. These findings suggest that the risk scores of COAD patients are great associated with subtype, TNM stage, lymph nodes, and distant metastases.

The degree of infiltration of 23 immune cell types with risk scores and 13 m^6A methylation-related prognostic lncRNA predictors were further analyzed to evalute the affect of risk scores on the tumor immune microenvironment of COAD and to explore the lncRNA predictors that play a mainly role in immune infiltration. The bubble map species showed the relationship between 13 methylation-related prognostic lncRNA predictors as well as risk scores with the degree of infiltration of 23 immune cells, respectively (Fig. 6F), with *LINC00861* having a higher correlation with the degree of 23 immune cell infiltration and a positive association with the degree of immune cell infiltration.

3.8 Construction and examination of Nomograms based on risk scores and clinical attributes

To determine whether risk score could be an independent prognostic factor for patients with COAD, single-factor and multifactor COX regression analyses were performed in the training and validation sets, respectively. In univariate analysis, TNM staging ($P < 0.001$) and risk score ($P < 0.001$) were significantly associated with OS in the TCGA training cohort. (Fig. 7A). TNM staging and risk score were then included in a multifactorial Cox regression analysis, which showed that TNM stage ($p < 0.001$) and risk score ($p < 0.001$) remained strongly associated with OS, and interestingly the results after excluding confounding showed that age was also an independent prognostic factor strongly associated with OS ($p = 0.002$) (Fig. 7B).

In the validation cohort, single-factor COX analysis showed that risk score ($p < 0.001$), TNM stage ($p < 0.001$), age ($p = 0.015$), and OS were highly correlated (Fig. 7C). Similarly, when these factors were included in the single-factor COX analysis, TNM stage ($p < 0.001$), risk score ($p < 0.001$), and age ($p = 0.003$) remained significantly associated with OS (Fig. 7D). The results showed that the risk score obtained from the expression levels of 13 m^6A methylation-related prognostic lncRNA predictors was an independent prognostic factor in patients with COAD.

Finally, we constructed a nomogram including risk scores and clinical attributes. The risk score, age, sex, and TNM stage were summed to calculate the total score (Fig. 7E). The calibration curves for predicting 1-year, 3-year, and 5-year OS showed that the survival predicted by the nomogram was closely related to the actual survival outcome. (Fig. 7F, G, H), and its AUC curves at 1, 3, and 5 years were 0.797, 0.826, and 0.808 higher than the clinical characteristics such as risk score alone with and TNM staging (Fig. 7I, J, K).

3.9 Genetic alterations in m^6A methylation-associated prognostic lncRNAs are associated with predictive markers

of immunotherapy efficacy

Patients with MSI-H received lower risk scores, whereas patients with COAD with MSI-L ($P < 0.01$) and MSS($P < 0.05$) received higher risk scores (Fig. 8A). We compared the tumor mutational burden of different risk scoring subgroups (Fig. 8B), compared with the low score group, the tumor mutation burden of the high-risk score group was lower. ($P < 0.05$).

We further conducteded SMG analysis on COAD samples from the low-risk scoring subgroup and the high-risk scoring subgroup (Fig. 8C). SMG mutation profiles showed that in addition to *TP53* (63% versus 43%, $P < 0.001$) and *APC* (81% versus 68%, $P < 0.01$) which had a higher somatic mutation rate in the high-risk scoring group, *FAT4*, *MUC16* ($P < 0.001$), *DNAH11*, *ABCA13* ($p < 0.05$) had higher somatic mutation rates in the low-risk score subgroup (Fisher's Exact test).

In addition to this, the IPS of *PD1* alone or in combination with *CTLA4* was higher in the low-risk scoring group than in the high-scoring group. (Fig. 8D and E) ($P < 0.05$). We continued to explore the differences in immune checkpoint expression in the risk score groups and found that *CD274* expression was significantly higher in the low-risk group. (Fig. 8F, $P < 0.05$)

3.10 Screening for sensitive drugs targeting high-risk genes in m^{6}A methylation-associated lncRNAs prognostic models

By performing CMAP drug sensitivity analysis of differential genes obtained from differential analysis of the high-risk scoring group combined with the low-risk scoring group in the prognostic model, we identified 32 sensitive drugs capable of inhibiting high-risk genes in the prognostic model grouping of m^{6}A-associated lncRNAs.

Among these drugs, piperidolate, quinostatin, and mecamylamine showed the highest degree of negative enrichment suggesting that these three drugs have the highest sensitivity to suppress high-risk genes in prognostic models. (all $p > 0.05$. Table 1).

Table 1
Predicted small molecules in CMAP

rank	cmap name	enrichment	p
1	piperidolate	-0.945	0.00028
2	quinostatin	-0.902	0.01927
3	mecamylamine	-0.876	0.00387
4	prenylamine	-0.845	0.00103
5	bezafibrate	-0.835	0.00131
6	chrysin	-0.824	0.01084
7	crotamiton	-0.8	0.0031
8	ebselen	-0.797	0.01719
9	gliclazide	-0.791	0.00386
10	etomidate	-0.789	0.01909
11	CP-645525-01	-0.746	0.03333
12	canavanine	-0.732	0.03992
13	bethanechol	-0.703	0.01593
14	sulconazole	-0.682	0.02234
15	scoulerine	-0.673	0.02572
16	oxybutynin	-0.671	0.0261
17	epitiostanol	-0.67	0.02668
18	levocabastine	-0.657	0.03149
19	halcinonide	-0.65	0.01278
20	parbendazole	-0.648	0.03621
21	phenoxybenzamine	-0.638	0.04144
22	cyclopenthiazide	-0.631	0.04563
23	dosulepin	-0.627	0.04794
24	suloctidil	-0.623	0.04999
25	edrophonium chloride	-0.576	0.04117
26	amprolium	-0.576	0.04133
27	cefazolin	-0.568	0.04558

rank	cmap name	enrichment	p
28	naloxone	-0.564	0.02576
29	cinchocaine	-0.562	0.04962
30	phenformin	-0.559	0.01335
31	metoclopramide	-0.524	0.04728
32	prochlorperazine	-0.511	0.00016

4. Discussion

The n6-methyladenosine (m6A) is the most enriched internal epigenetic modification in eukaryotic mRNA. [23]. In terms of molecular mechanisms, m6A is involved in nearly every step of RNA metabolism, including translation, degradation, splicing, export, folding of mRNA [24], and processing of mRNA and non-coding RNA (ncRNA) [9]. We found alterations in m^6A levels are involved in cancer pathogenesis and development by modulating the expression of tumor-associated genes. The effects of lncRNA in tumors is not uniform, with some acting as carcinogens and others as tumor suppressors, whose aberrant expression, mutations and SNPs are closely associated with tumorigenesis and metastasis [25, 26].

There has been increasing evidence that m^6A modifications interact with lncRNAs as an important link affecting tumor development. For example, long-stranded non-coding RNA FAM225A drives nasopharyngeal carcinogenesis and metastasis via its role as a ceRNA for sponge miR-590-3p/miR-1275 and upregulation of ITGB3 [27]. Wu et al. found m^6A -inducible lncRNAs *RP11* induces the propagation of colorectal cancer cells by upregulating Zeb1[28].Wang et al. believed lncRNA *LINRIS* protects *IGF2BP2* by stabilizing it and promoting aerobic glycolysis in colorectal cancer [29]. In addition, Ni et al. found the long-stranded non-coding RNA *GAS5* interacts with *YAP* and triggers *its* phosphorylation and degradation to inhibit colorectal cancer progression, which is under negative regulation by the m^6A reader *YTHDF3*[30]. However, the overall characteristics of TME mediated by the interaction of m^6A with lncRNAs and their impact on therapy and prognosis still lack a comprehensive understanding. Therefore, identifying the mode of action of different m6A-related lncRNAs in the tumor immune microenvironment can provide deeper understanding of the effect of m6A-lncRNA interactions in anti-tumor immune responses, as well as the tumor prognostic features of COAD mediated by m6A-related lncRNAs, which will help develop more effective and precise immunotherapeutic strategies.

We demonstrated the expression and prognostic value of m6A-associated prognostic lncRNAs in COAD, as well as their association with tumor immune microenvironment and ICI therapy. Subsequently, we built a prognostic module on the basis of m6A-associated prognostic lncRNAs, and screened sensitive drugs targeting high-risk genes.

The 43 m^6A-associated prognostic lncRNAs we detected were all prognostic risk factors for COAD and differed significantly in both COAD tumors and normal paracancerous tissues. Among them, *SNHG26*, *AC145285.2*, *AC026367.1*, *AC092944.1*, *GLIDR*, *AL512306.3*, *U91328.1*, *ATP2B1-AS1*, *PRKAR1B-AS2*, *SEPTIN7-DT*, *AC104819.3*, *NIFK-AS1*, *AC019205.1*, *LINC01588*, *LINC00861* had significantly lower expression in COAD tissues. The rest are highly expressed in COAD.

We also made a comparison of the expression differences of eight common immune checkpoints in COAD tumor tissues and paraneoplastic tissues and found that they were not consistently expressed. This suggests that the expression of these immune checkpoints differs between cancer and normal tissues, and also suggests that there are differences in immune checkpoint expression between individual COAD patients, and that clarifying these differences and using different immune checkpoint treatments may bring different benefits to patients, and continuing to explore the differences in immune checkpoint expression between different subgroups facilitates more effective individualized treatment.

The differences in tumor immune microenvironment (TIME) between subtypes of clusters A, B, and C were significant. clusters A and C with good prognosis both had significantly higher immune scores than cluster B. The emarkable difference in survival rates between clusters A and C may be correlated to the higher immunization scores in clusters A and C. However cluster A did not outperform the other two groups in assessing the IPS score for immunotherapy, which may be due to the complex TME effect.

Immune and stromal cells are affected by tumor cell and TME interactions and can contribute in part to tumor development[31]. TME components and immune system biomarkers are of importance for cancer detection, prognostic assessment, and therapeutic response[32]. The tumor-related mesenchyme provides nutrients, oxygen, enzymes, and stroma-bound growth factors, which promote tumor progression and proliferation[31–33].

Further analysis suggested that the infiltration of 23 immune cell types was generally higher in group A than in groups B and C. However, this also included some immunosuppressive cells such as Treg and MDSC, and some stroma-related expression was also higher in group A than in groups B and C. Recent studies have previously shown that immune cells prefer keeping in the stroma around the tumor cell nests than penetrating the parenchyma of the tumor cells, a phenotype also known as the immune rejection phenotype[34]. In addition, multiple immunosuppressive immune cells are commonly found in TME of colorectal cancer. MDSCs are proven immunosuppressive cells, which are similar to queen bees, can promote the formation of Tregs [35]. Besides, MDSCs often become TAMs[36] and facilitate the differentiation of fibroblasts into CAFs[37], even shadowing the risk of death in tumor-ridden patients and increasing the risk of checkpoint inhibitor (CPI) resistance [38, 39]. Similar to MDSCs, the role of regulatory T cells (Tregs) in colorectal cancer has not been fully elucidated. Treg participates in effector t cell-mediated inflammation suppression through various mechanisms, including the release of transforming growth factor-β and interleukin-10 [40]. The mean content of Tregs in the blood in colorectal cancer is higher than that of healthy volunteers. The average content of Tregs in tumor is higher than that in adjacent non-tumor[41]. In addition, many studies have shown that Tregs in tumor can inhibit the

proliferation of autologous $CD4^+$ and $CD8^+$ T cells [42], and the frequency of Tregs is negatively correlated with the expression of IFN-γ and IL-2 in tumor tissues [43]. Hence, some studies suggested they are associated with poor prognosis[44].

Hence, we hypothesized that the higher immune score in cluster A, but not better IPS score and OS than the other two clusters, may be the result of the retention of immune cells in the stroma around the tumor cell nests and immune tolerance induced by immunosuppressive cells that do not fully exert immunocidal effects.

GSVA results suggest the presence of downregulation of cancer suppressor pathways including P53, and apoptosis in cluster B. P53 is an important tumor suppressor encoded by the oncogene *TP53* and is involved in many vital biological procedures including cell cycle arrest, senescence, and apoptosis[45, 46]. P53 has also recently been shown to regulate cellular metabolism maintaining intracellular iron homeostasis and drive iron death to inhibit tumor development [47–49], while perturbative deletion or mutation of P53 regulates immune recognition and thus promotes an immunosuppressive environment through mechanisms such as reduced MHC-I presentation and increased suppressive myeloid cells and Treg [14]. This may be an important reason for the lower OS in the cluster B group compared to the remaining two groups.

In addition to P53 pathway, some immune-related pathways are activated in cluster C but exhibit inactivation in cluster B, such as interferon-α responses.

The IFNα pathway has been shown to assist the signaling cascade by boosting the expression of IL21,IFN-γ, IL15[20, 50, 51]and other cytokines in immune cells to drive the maturation of DCs[21], which differentiated $CD4^+$ T cells into Th1 [22] and increased the activation and cytotoxicity of $CD8^+$ T cells[52]. IFNα has also been shown to mediate these immunomodulatory roles also in the absence of reliance on intermediate cytokine production[21]. This is consistent with previous results that differences in interferon-alpha response may be responsible for differences in cluster A and C immune cell infiltration as well as prolonged OS.

Cluster A, however, exhibits paradoxical antitumor immunity, with both enrichment of antitumor immune cells and enrichment of Treg and MDSCs mediating immunosuppression, with both the highest immune and stromal scores.

Previous studies have shown that IL2 activation of STAT5 induces Foxp3 to sustain regulatory T cell development[53–55], while activation of EMT and transforming growth factor-β-related pathways impedes lymphocyte infiltration into the tumor parenchyma[56]. This may account for Treg enrichment and mesenchymal activation in cluster A. Immune checkpoint blockade (ICB) combination therapy targeting these immunosuppressive mechanisms may improve the outcome of patients in cluster A and further prolong OS[57, 58].

We evaluated the prognostic value of m^6A-related prognostic lncRNAs in COAD patients and derived 13 prognostic risk signals from them. The risk signals effectively classified COAD patients into two groups: high-risk and low-risk. In the TCGA training and validation cohort, patients in the high-risk group had significantly shorter OS than those in the low-risk group. Among these predictors, some have been reported, such as silencing of *ATP2B1-AS1* that blocks *NFKBIA*-mediated *NF-κB* signaling pathway[59], *LINC00861* as a protective factor in ovarian cancer, as a ceRNA for *miR-513b-5p* in cervical cancer, regulating PTEN/AKT/mTOR signaling pathway to inhibit cervical cancer cell progression, and Closely associated with *PD1*, *PD-L1* and *CTLA4* in prostate cancer[60–62]. *AC003101.2* was predicted to play a ceRNA role in colorectal cancer[63], and *AC156455.1* was reported to be a prognostic predictor associated with genomic instability in renal clear cell carcinoma[64]. *AC005229.4* was also reported to be an autophagy-related prognostic indicator in hepatocellular carcinoma, bladder cancer and endometrial cancer [65–67].

Moreover, linking the risk score and clinical attributes that we create a nomogram and examined it using data from TCGA, which has a great capacity to predict OS in COAD patients beneficially helping us to predict patient survival and clinical decision making.

Transforming growth factor β receptor II (*TGFβRII*), encoding β-catenin (*CTNNB1*), epidermal growth factor receptor (*EGFR*), And bcl-2-associated x protein (*bax*), which can encode microsatellite, often mutates in dMMR/MSI CRC[4]. It has been shown that patients with dMMR/MSI early COAD have a better prognosis and survival compared to patients with pMMR/MSI mutations[18, 68], in addition, tumors possessing these features typically have a higher density of tumor-infiltrating lymphocytes (TIL) than MSS tumors, possess a stronger anti-tumor immune response[69, 70], and are more sensitive to ICIs sensitive to ICIs, which may be due to a large number of new tumor antigens produced by MSI CRC, which is caused by the mutation of synthetic truncated protein caused by unrepaired frameshift mutation [71]. There is an overlap between MSI-H/dMMR and tumors with high TMB, but a large proportion of CRC with high TMB does not have defects in the MMR pathway, making TMB a more inclusive biomarker and thus greatly increasing the number of potential patients who may be identified as good candidates for ICI therapy[72]. However, TMB assessments are more expensive, the standardization of TMB scoring needs to be further improved, and the applicability of the predicted values to MS/pMMR still needs to be evaluated[73].

We, therefore, continued to explore the TMB, MSI, and IPS characteristics of COAD patients in the risk score group, and our study found that TMB was higher in the low-risk score group, and risk scores were lower in COAD patients with MSI-H status, and that *PD1* or *PD1* combined with *CTLA4* had a better effect in the IPS prediction in the low-risk score group. This is consistent with some previously reported results, which implies that these 13 lncRNAs could influence the efficacy of immunotherapy and could be used as a surrogate for improving patient stratification and assessing the effectiveness of immunotherapy. In addition, we valuated the top 20 most mutated genes in COAD and found that the mutation frequency was upper in the low-risk group overall, except for tumor suppressor genes such as *TP53* and *APC*, which

had a higher mutation frequency in the high-risk group, which was consistent with the previous GSVA analysis.

In addition, the combination of TMB with other biomarkers, such as immune checkpoints, may be more effective in forecasting the therapeutic efficacy of immunotherapy and provide guidance for clinical practice, so we proceeded to compare the differences in immune checkpoint expression between the high-risk scoring group and the low-risk scoring group. We observed that the expression of the immune checkpoint *CD274* was higher in the low-risk scoring group than in the high-risk scoring group. The results based on IPS scores as well as TMB and the differential expression of *CD274* also suggest that m^6A-related lncRNAs may be able to guide individual patient treatment strategies and improve stratification of ICB therapy in COAD patients.

The tumor microenvironment plays an important regulatory role in tumorigenesis, which is regulated by lncRNAs during dynamic changes. This has been demonstrated in previous studies, for example, lncRNA MALAT1 was previously shown to adsorb miR195 to promote the development of diffuse large B-cell lymphoma and immune escape. In addition to this, lncRNA UCA1 overexpression protects PDL1 expression from miRNA inhibition and promotes immune escape in gastric adenocarcinoma cells [74-75].

However, current tumor knowledge of m^6A-associated prognostic lncRNAs in COAD remains limited. In the present study, the risk scores of 13 prognostic predictors constructed based on m^6A-related prognostic lncRNAs were inconsistently associated with 23 immune cell infiltration. *LINC00861*, *ATP2B1-AS1* were mainly positively associated with immune cell infiltration, but the other predictors were overall negatively correction with the infiltration of immune cell. This may explain the lack of difference in immune scores between the high-risk and low-risk score groups.

In addition we screened for sensitive drugs that can inhibit high-risk genes in prognostic models of m^6A-related lncRNAs, such as quinostatin, mecamylamine, and piperidolate .The ability of quinostatin to inhibit the PI3K-MTOR pathway is probably significant for its anti-tumor role[76]. And mecamylamine inhibits the α7nAChR/NF-κB p100/p52 pathway, promotes apoptosis and disrupts the anti-inflammatory effect in macrophages, perhaps also taking the corresponding effect in the treatment of COAD[77]. Piperidolate is an anticholinergic agent, and previous studies have demonstrated that inhibition of cholinergic receptors can inhibit the proliferation of a variety of cancers, suggesting a potential role for piperidolate in oncology treatment[78].

This study was validated only in the TCGA dataset, which has limitations. Further and more independent COAD cohorts should be utilized to confirm the role of the detected m^6A-related prognosis-related lncRNAs for prognostic stratification of COAD. Moreover, the role and mechanism of m^6A-related lncRNAs for TME as well as COAD development still need to be proved in vitro and vivo. Our results may contribute to provide some usable clues for further experimental studies.

5. Conclusion

This study highlights that m6A-related lncRNAs are significantly associated with TME as well as immune response. Quantitative assessment of m6A-associated lncRNAs in individual tumors will enhance our understanding of the TME profile and immune checkpoint expression profile. m6A-associated lncRNAs constructed a prognostic model that facilitates prognosis and immunotherapy stratification in COAD patients, and based on the model we screened three drugs with potential therapeutic value.

Abbreviations

m6A: N6-methyladenosine; TME: tumor microenvironment; COAD: colon adenocarcinoma; CRC: colorectal cancer; ssGSEA: Single sample gene set enrichment analysis; Lasso: least absolute shrinkage and selection operator; MSI: microsatellite instability; IPS: immunophenotypic score; TMB: tumor mutation burden; *FAT4*: FAT Atypical Cadherin 4; *MUC16*: Mucin 16; lncRNA: Long non-coding RNA; PD-1: programmed death receptor 1; PD-L1: programmed cell death 1 ligand 1; mRNA: messenger RNA; ncRNA: non-coding RNA; TCGA: The Cancer Genome Atlas; *RBM15B*: RNA Binding Motif Protein 15B; *ALKBH5*: AlkB Homolog 5; *PDCD1LG2*: Programmed Cell Death 1 Ligand 2; *LAG3*: Lymphocyte Activating 3; *SIGLEC15*: Sialic Acid Binding Ig Like Lectin 15; *CTLA4*: Cytotoxic T-Lymphocyte Associated Protein 4; *CD274*: Programmed Cell Death 1 Ligand 1; *TP53*: Tumor Protein P53; *APC*: APC Regulator Of WNT Signaling Pathway; *DNAH11*: Dynein Axonemal Heavy Chain 11; *ABCA13*: ATP Binding Cassette Subfamily A Member 13; PCA: principal component analysis; AUC: the area under receiver operating characteristic curve; ROC: receiver operating characteristic; OS: over survival; Treg: Regulatory T cells; MDSCs: Myeloid-derived suppressor cells; GSVA: Gene set variation analysis; ICI: immune check-point inhibitors; ICB: immune-checkpoint blockade. TIL: tumor-infiltrating lymphocytes; dMMR: Mismatch repair deficiency; pMMR: Mismatch repair proficiency; ceRNA: competing endogenous RNAs; CMAP: Connectivity map; Degs: Differentially expressed genes.

Declarations

Acknowledgments: This work was supported by the Guangxi Natural Science Foundation project (2018GXNSFAA281129; project recipient: Liu Zhihui).

Funding: Guangxi Natural Science Foundation Project (2018GXNSFAA281129).

Authors' contributions: HLW, ZYH, ZMY performed most of the investigation, data analysis and wrote the manuscript; ZHL and LH contributed to the interpretation of data analysis and editing of the article.

Availability of data and materials: The data could be download at (https://tcia.at/home and https://tcia.at/home), and the code used during the current study are available from the corresponding author on reasonable request.

All of the authors have read and approved the manuscript.

Ethics approval and consent to participate: Not applicable

Patient consent for publication: Not applicable

Competing interests: The authors declare that they have no competing interests, and all authors should confirm its accuracy.

References

1. Mayer RJ: **Systemic therapy for colorectal cancer: an overview**. *Semin Oncol* 1991, **18**(5 Suppl 7):62-66.
2. Markowitz SD, Bertagnolli MM: **Molecular origins of cancer: Molecular basis of colorectal cancer**. *N Engl J Med* 2009, **361**(25):2449-2460.
3. Li Z, Tan H, Yu H, Deng Z, Zhou X, Wang M: **DNA methylation and gene expression profiles characterize epigenetic regulation of lncRNAs in colon adenocarcinoma**. *J Cell Biochem* 2020, **121**(3):2406-2415.
4. Vogelstein B, Papadopoulos N, Velculescu VE, Zhou S, Diaz LA, Jr., Kinzler KW: **Cancer genome landscapes**. *Science* 2013, **339**(6127):1546-1558.
5. Arneth B: **Tumor Microenvironment**. *Medicina (Kaunas)* 2019, **56**(1).
6. Le DT, Uram JN, Wang H, Bartlett BR, Kemberling H, Eyring AD, Skora AD, Luber BS, Azad NS, Laheru D *et al*: **PD-1 Blockade in Tumors with Mismatch-Repair Deficiency**. *N Engl J Med* 2015, **372**(26):2509-2520.
7. Germano G, Lamba S, Rospo G, Barault L, Magri A, Maione F, Russo M, Crisafulli G, Bartolini A, Lerda G *et al*: **Inactivation of DNA repair triggers neoantigen generation and impairs tumour growth**. *Nature* 2017, **552**(7683):116-120.
8. Bray F, Ferlay J, Soerjomataram I, Siegel RL, Torre LA, Jemal A: **Global cancer statistics 2018: GLOBOCAN estimates of incidence and mortality worldwide for 36 cancers in 185 countries**. *CA Cancer J Clin* 2018, **68**(6):394-424.
9. Huang H, Weng H, Chen J: **m(6)A Modification in Coding and Non-coding RNAs: Roles and Therapeutic Implications in Cancer**. *Cancer Cell* 2020, **37**(3):270-288.
10. Ban Y, Tan P, Cai J, Li J, Hu M, Zhou Y, Mei Y, Tan Y, Li X, Zeng Z *et al*: **LNCAROD is stabilized by m6A methylation and promotes cancer progression via forming a ternary complex with HSPA1A and YBX1 in head and neck squamous cell carcinoma**. *Mol Oncol* 2020, **14**(6):1282-1296.
11. Tu Z, Wu L, Wang P, Hu Q, Tao C, Li K, Huang K, Zhu X: **N6-Methylandenosine-Related lncRNAs Are Potential Biomarkers for Predicting the Overall Survival of Lower-Grade Glioma Patients**. *Front Cell Dev Biol* 2020, **8**:642.
12. Chen T, Hao YJ, Zhang Y, Li MM, Wang M, Han W, Wu Y, Lv Y, Hao J, Wang L *et al*: **m(6)A RNA methylation is regulated by microRNAs and promotes reprogramming to pluripotency**. *Cell stem cell* 2015, **16**(3):289-301.

13. Zhang C, Chen Y, Sun B, Wang L, Yang Y, Ma D, Lv J, Heng J, Ding Y, Xue Y *et al*: **m(6)A modulates haematopoietic stem and progenitor cell specification**. *Nature* 2017, **549**(7671):273-276.
14. Blagih J, Buck MD, Vousden KH: **p53, cancer and the immune response**. *Journal of cell science* 2020, **133**(5).
15. Curtsinger JM, Agarwal P, Lins DC, Mescher MF: **Autocrine IFN-¦Ã promotes naive CD8 T cell differentiation and synergizes with IFN-¦Á to stimulate strong function**. *Journal of immunology (Baltimore, Md : 1950)* 2012, **189**(2):659-668.
16. Haabeth OA, Lorvik KB, Hammarstr?m C, Donaldson IM, Haraldsen G, Bogen B, Corthay A: **Inflammation driven by tumour-specific Th1 cells protects against B-cell cancer**. *Nature communications* 2011, **2**:240.
17. Nathan CF, Murray HW, Wiebe ME, Rubin BY: **Identification of interferon-gamma as the lymphokine that activates human macrophage oxidative metabolism and antimicrobial activity**. *The Journal of experimental medicine* 1983, **158**(3):670-689.
18. Boland CR, Goel A: **Microsatellite instability in colorectal cancer**. *Gastroenterology* 2010, **138**(6):2073-2087.e2073.
19. Sadlik JR, Hoyer M, Leyko MA, Horvat R, Parmely M, Whitacre C, Zwilling B, Rinehart JJ: **Lymphocyte supernatant-induced human monocyte tumoricidal activity: dependence on the presence of gamma-interferon**. *Cancer research* 1985, **45**(5):1940-1945.
20. Mattei F, Schiavoni G, Belardelli F, Tough DF: **IL-15 is expressed by dendritic cells in response to type I IFN, double-stranded RNA, or lipopolysaccharide and promotes dendritic cell activation**. *Journal of immunology (Baltimore, Md : 1950)* 2001, **167**(3):1179-1187.
21. Montoya M, Schiavoni G, Mattei F, Gresser I, Belardelli F, Borrow P, Tough DF: **Type I interferons produced by dendritic cells promote their phenotypic and functional activation**. *Blood* 2002, **99**(9):3263-3271.
22. Rogge L, Ambrosio D, Biffi M, Penna G, Minetti LJ, Presky DH, Adorini L, Sinigaglia F: **The role of Stat4 in species-specific regulation of Th cell development by type I IFNs**. *Journal of immunology (Baltimore, Md : 1950)* 1998, **161**(12):6567-6574.
23. Yue Y, Liu J, He C: **RNA N6-methyladenosine methylation in post-transcriptional gene expression regulation**. *Genes & development* 2015, **29**(13):1343-1355.
24. Liu Q, Gregory RI: **RNAmod: an integrated system for the annotation of mRNA modifications**. *Nucleic acids research* 2019, **47**(W1):W548-W555.
25. Bhan A, Soleimani M, Mandal SS: **Long Noncoding RNA and Cancer: A New Paradigm**. *Cancer research* 2017, **77**(15):3965-3981.
26. Baldassarre A, Masotti A: **Long non-coding RNAs and p53 regulation**. *International journal of molecular sciences* 2012, **13**(12):16708-16717.
27. Zheng ZQ, Li ZX, Zhou GQ, Lin L, Zhang LL, Lv JW, Huang XD, Liu RQ, Chen F, He XJ *et al*: **Long Noncoding RNA FAM225A Promotes Nasopharyngeal Carcinoma Tumorigenesis and Metastasis by**

Acting as ceRNA to Sponge miR-590-3p/miR-1275 and Upregulate ITGB3. *Cancer research* 2019, **79**(18):4612-4626.

28. Wu Y, Yang X, Chen Z, Tian L, Jiang G, Chen F, Li J, An P, Lu L, Luo N *et al*: **m(6)A-induced lncRNA RP11 triggers the dissemination of colorectal cancer cells via upregulation of Zeb1**. *Molecular cancer* 2019, **18**(1):87.
29. Wang Y, Lu JH, Wu QN, Jin Y, Wang DS, Chen YX, Liu J, Luo XJ, Meng Q, Pu HY *et al*: **LncRNA LINRIS stabilizes IGF2BP2 and promotes the aerobic glycolysis in colorectal cancer**. *Molecular cancer* 2019, **18**(1):174.
30. Ni W, Yao S, Zhou Y, Liu Y, Huang P, Zhou A, Liu J, Che L, Li J: **Long noncoding RNA GAS5 inhibits progression of colorectal cancer by interacting with and triggering YAP phosphorylation and degradation and is negatively regulated by the m(6)A reader YTHDF3**. *Molecular cancer* 2019, **18**(1):143.
31. Watnick RS: **The role of the tumor microenvironment in regulating angiogenesis**. *Cold Spring Harb Perspect Med* 2012, **2**(12):a006676.
32. Angell H, Galon J: **From the immune contexture to the Immunoscore: the role of prognostic and predictive immune markers in cancer**. *Curr Opin Immunol* 2013, **25**(2):261-267.
33. Pottier C, Wheatherspoon A, Roncarati P, Longuesp¨¦e R, Herfs M, Duray A, Delvenne P, Quatresooz P: **The importance of the tumor microenvironment in the therapeutic management of cancer**. *Expert review of anticancer therapy* 2015, **15**(8):943-954.
34. Chen DS, Mellman I: **Elements of cancer immunity and the cancer-immune set point**. *Nature* 2017, **541**(7637):321-330.
35. Ugel S, De Sanctis F, Mandruzzato S, Bronte V: **Tumor-induced myeloid deviation: when myeloid-derived suppressor cells meet tumor-associated macrophages**. *The Journal of clinical investigation* 2015, **125**(9):3365-3376.
36. Veglia F, Perego M, Gabrilovich D: **Myeloid-derived suppressor cells coming of age**. *Nature immunology* 2018, **19**(2):108-119.
37. Alkasalias T, Moyano-Galceran L, Arsenian-Henriksson M, Lehti K: **Fibroblasts in the Tumor Microenvironment: Shield or Spear?** *International journal of molecular sciences* 2018, **19**(5).
38. Martens A, Wistuba-Hamprecht K, Geukes Foppen M, Yuan J, Postow MA, Wong P, Romano E, Khammari A, Dreno B, Capone M *et al*: **Baseline Peripheral Blood Biomarkers Associated with Clinical Outcome of Advanced Melanoma Patients Treated with Ipilimumab**. *Clinical cancer research : an official journal of the American Association for Cancer Research* 2016, **22**(12):2908-2918.
39. Gonda K, Shibata M, Ohtake T, Matsumoto Y, Tachibana K, Abe N, Ohto H, Sakurai K, Takenoshita S: **Myeloid-derived suppressor cells are increased and correlated with type 2 immune responses, malnutrition, inflammation, and poor prognosis in patients with breast cancer**. *Oncology letters* 2017, **14**(2):1766-1774.
40. Yamamoto H, Imai K: **Microsatellite instability: an update**. *Arch Toxicol* 2015, **89**(6):899-921.

41. Saeterdal I, Bjorheim J, Lislerud K, Gjertsen MK, Bukholm IK, Olsen OC, Nesland JM, Eriksen JA, Moller M, Lindblom A *et al*: **Frameshift-mutation-derived peptides as tumor-specific antigens in inherited and spontaneous colorectal cancer**. *Proc Natl Acad Sci U S A* 2001, **98**(23):13255-13260.
42. Laghi L, Bianchi P, Delconte G, Celesti G, Di Caro G, Pedroni M, Chiaravalli AM, Jung B, Capella C, de Leon MP *et al*: **MSH3 protein expression and nodal status in MLH1-deficient colorectal cancers**. *Clin Cancer Res* 2012, **18**(11):3142-3153.
43. Dienstmann R, Vermeulen L, Guinney J, Kopetz S, Tejpar S, Tabernero J: **Consensus molecular subtypes and the evolution of precision medicine in colorectal cancer**. *Nat Rev Cancer* 2017, **17**(2):79-92.
44. Giannakis M, Mu XJ, Shukla SA, Qian ZR, Cohen O, Nishihara R, Bahl S, Cao Y, Amin-Mansour A, Yamauchi M *et al*: **Genomic Correlates of Immune-Cell Infiltrates in Colorectal Carcinoma**. *Cell Rep* 2016, **17**(4):1206.
45. Levine AJ, Oren M: **The first 30 years of p53: growing ever more complex**. *Nature reviews Cancer* 2009, **9**(10):749-758.
46. Levine AJ, Hu W, Feng Z: **The P53 pathway: what questions remain to be explored?** *Cell death and differentiation* 2006, **13**(6):1027-1036.
47. Gnanapradeepan K, Basu S, Barnoud T, Budina-Kolomets A, Kung CP, Murphy ME: **The p53 Tumor Suppressor in the Control of Metabolism and Ferroptosis**. *Frontiers in endocrinology* 2018, **9**:124.
48. Funauchi Y, Tanikawa C, Yi Lo PH, Mori J, Daigo Y, Takano A, Miyagi Y, Okawa A, Nakamura Y, Matsuda K: **Regulation of iron homeostasis by the p53-ISCU pathway**. *Scientific reports* 2015, **5**:16497.
49. Zhang Y, Qian Y, Zhang J, Yan W, Jung YS, Chen M, Huang E, Lloyd K, Duan Y, Wang J *et al*: **Ferredoxin reductase is critical for p53-dependent tumor suppression via iron regulatory protein 2**. *Genes & development* 2017, **31**(12):1243-1256.
50. Strengell M, Julkunen I, Matikainen S: **IFN-alpha regulates IL-21 and IL-21R expression in human NK and T cells**. *Journal of leukocyte biology* 2004, **76**(2):416-422.
51. Byrnes AA, Ma X, Cuomo P, Park K, Wahl L, Wolf SF, Zhou H, Trinchieri G, Karp CL: **Type I interferons and IL-12: convergence and cross-regulation among mediators of cellular immunity**. *European journal of immunology* 2001, **31**(7):2026-2034.
52. Fuertes MB, Kacha AK, Kline J, Woo SR, Kranz DM, Murphy KM, Gajewski TF: **Host type I IFN signals are required for antitumor CD8+ T cell responses through CD8{alpha}+ dendritic cells**. *The Journal of experimental medicine* 2011, **208**(10):2005-2016.
53. Feng Y, Arvey A, Chinen T, van der Veeken J, Gasteiger G, Rudensky AY: **Control of the inheritance of regulatory T cell identity by a cis element in the Foxp3 locus**. *Cell* 2014, **158**(4):749-763.
54. Josefowicz SZ, Lu LF, Rudensky AY: **Regulatory T cells: mechanisms of differentiation and function**. *Annual review of immunology* 2012, **30**:531-564.
55. Nasrallah R, Imianowski CJ, Bossini-Castillo L, Grant FM, Dogan M, Placek L, Kozhaya L, Kuo P, Sadiyah F, Whiteside SK *et al*: **A distal enhancer at risk locus 11q13.5 promotes suppression of colitis**

by T(reg) cells. *Nature* 2020, **583**(7816):447-452.

56. Tauriello DVF, Palomo-Ponce S, Stork D, Berenguer-Llergo A, Badia-Ramentol J, Iglesias M, Sevillano M, Ibiza S, Ca?ellas A, Hernando-Momblona X *et al*: **TGF¦Â drives immune evasion in genetically reconstituted colon cancer metastasis**. *Nature* 2018, **554**(7693):538-543.
57. Panagi M, Voutouri C, Mpekris F, Papageorgis P, Martin MR, Martin JD, Demetriou P, Pierides C, Polydorou C, Stylianou A *et al*: **TGF-¦Â inhibition combined with cytotoxic nanomedicine normalizes triple negative breast cancer microenvironment towards anti-tumor immunity**. *Theranostics* 2020, **10**(4):1910-1922.
58. Rani A, Murphy JJ: **STAT5 in Cancer and Immunity**. *Journal of interferon & cytokine research : the official journal of the International Society for Interferon and Cytokine Research* 2016, **36**(4):226-237.
59. Song KY, Zhang XZ, Li F, Ji QR: **Silencing of ATP2B1-AS1 contributes to protection against myocardial infarction in mouse via blocking NFKBIA-mediated NF-¦ÊB signalling pathway**. *Journal of cellular and molecular medicine* 2020, **24**(8):4466-4479.
60. Hu W, Wang Y, Fang Z, He W, Li S: **Integrated Characterization of lncRNA-Immune Interactions in Prostate Cancer**. *Frontiers in cell and developmental biology* 2021, **9**:641891.
61. Liu H, Zhang L, Ding X, Sui X: **LINC00861 inhibits the progression of cervical cancer cells by functioning as a ceRNA for miR?513b?5p and regulating the PTEN/AKT/mTOR signaling pathway**. *Molecular medicine reports* 2021, **23**(1).
62. Zheng M, Hu Y, Gou R, Nie X, Li X, Liu J, Lin B: **Identification three LncRNA prognostic signature of ovarian cancer based on genome-wide copy number variation**. *Biomedicine & pharmacotherapy = Biomedecine & pharmacotherapie* 2020, **124**:109810.
63. Wang X, Zhou J, Xu M, Yan Y, Huang L, Kuang Y, Liu Y, Li P, Zheng W, Liu H *et al*: **A 15-lncRNA signature predicts survival and functions as a ceRNA in patients with colorectal cancer**. *Cancer management and research* 2018, **10**:5799-5806.
64. Yang H, Xiong X, Li H: **Development and Interpretation of a Genomic Instability Derived lncRNAs Based Risk Signature as a Predictor of Prognosis for Clear Cell Renal Cell Carcinoma Patients**. *Frontiers in oncology* 2021, **11**:678253.
65. Jia Y, Chen Y, Liu J: **Prognosis-Predictive Signature and Nomogram Based on Autophagy-Related Long Non-coding RNAs for Hepatocellular Carcinoma**. *Frontiers in genetics* 2020, **11**:608668.
66. Wan J, Guo C, Fang H, Xu Z, Hu Y, Luo Y: **Autophagy-Related Long Non-coding RNA Is a Prognostic Indicator for Bladder Cancer**. *Frontiers in oncology* 2021, **11**:647236.
67. Wang X, Dai C, Ye M, Wang J, Lin W, Li R: **Prognostic value of an autophagy-related long-noncoding-RNA signature for endometrial cancer**. *Aging* 2021, **13**(4):5104-5119.
68. Popat S, Hubner R, Houlston RS: **Systematic review of microsatellite instability and colorectal cancer prognosis**. *Journal of clinical oncology : official journal of the American Society of Clinical Oncology* 2005, **23**(3):609-618.
69. Willis JA, Reyes-Uribe L, Chang K, Lipkin SM, Vilar E: **Immune Activation in Mismatch Repair-Deficient Carcinogenesis: More Than Just Mutational Rate**. *Clinical cancer research : an official journal of the*

American Association for Cancer Research 2020, **26**(1):11-17.

70. Turajlic S, Litchfield K, Xu H, Rosenthal R, McGranahan N, Reading JL, Wong YNS, Rowan A, Kanu N, Al Bakir M *et al*: **Insertion-and-deletion-derived tumour-specific neoantigens and the immunogenic phenotype: a pan-cancer analysis**. *Lancet Oncol* 2017, **18**(8):1009-1021.
71. Galon J, Costes A, Sanchez-Cabo F, Kirilovsky A, Mlecnik B, Lagorce-Pages C, Tosolini M, Camus M, Berger A, Wind P *et al*: **Type, density, and location of immune cells within human colorectal tumors predict clinical outcome**. *Science* 2006, **313**(5795):1960-1964.
72. Ritterhouse LL: **Tumor mutational burden**. *Cancer cytopathology* 2019, **127**(12):735-736.
73. Cohen R, Rousseau B, Vidal J, Colle R, Diaz LA, Jr., Andr¨¦ T: **Immune Checkpoint Inhibition in Colorectal Cancer: Microsatellite Instability and Beyond**. *Targeted oncology* 2020, **15**(1):11-24.
74. Wang QM, Lian GY, Song Y, Huang YF, Gong Y: **LncRNA MALAT1 promotes tumorigenesis and immune escape of diffuse large B cell lymphoma by sponging miR-195**. *Life sciences* 2019, **231**:116335.
75. Wang CJ, Zhu CC, Xu J, Wang M, Zhao WY, Liu Q, Zhao G, Zhang ZZ: **The lncRNA UCA1 promotes proliferation, migration, immune escape and inhibits apoptosis in gastric cancer by sponging anti-tumor miRNAs**. *Molecular cancer* 2019, **18**(1):115.
76. Yang J, Shamji A, Matchacheep S, Schreiber SL: **Identification of a small-molecule inhibitor of class Ia PI3Ks with cell-based screening**. *Chemistry & biology* 2007, **14**(4):371-377.
77. AlQasrawi D, Naser E, Naser SA: **Nicotine Increases Macrophage Survival through ¦Á7nAChR/NF-¦ÊB Pathway in Mycobacterium?avium?paratuberculosis Infection**. *Microorganisms* 2021, **9**(5).
78. Russo P, Del Bufalo A, Milic M, Salinaro G, Fini M, Cesario A: **Cholinergic receptors as target for cancer therapy in a systems medicine perspective**. *Current molecular medicine* 2014, **14**(9):1126-1138.

Figures

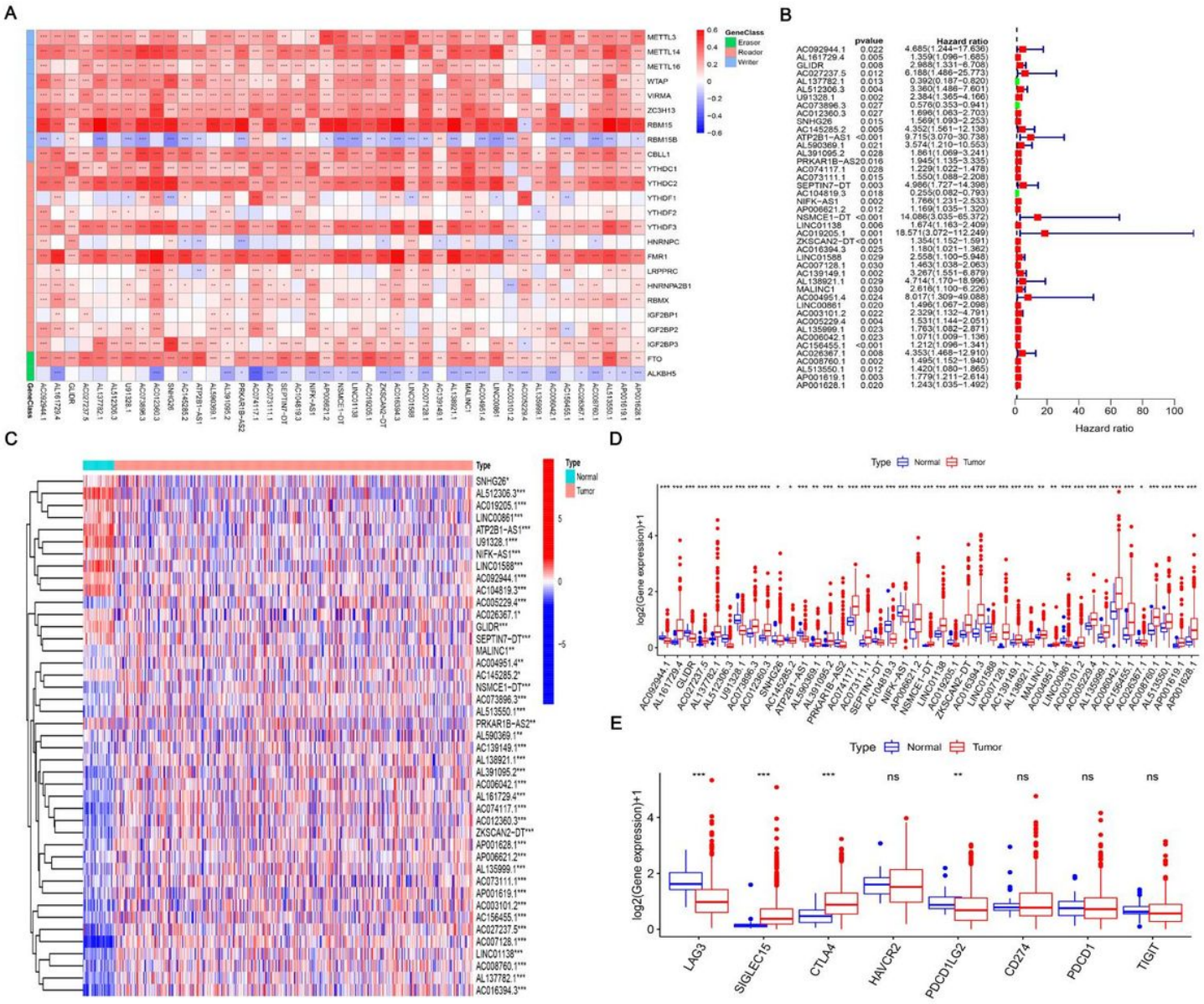

Figure 1

Correlation and survival risk ratio of 43 m^{6}A-associated prognostic lncRNAs with m^{6}A regulators. As well as differential analysis of 43 m^{6}A-associated prognostic lncRNAs and immune checkpoint expression levels in COAD and adjacent normal samples.

(A) Heat map of correlations between m^{6}A regulators and 43 m^{6}A-associated lncRNAs that predict prognosis. (B) Survival risk ratios of 43 m^{6}A-associated prognostic lncRNAs. (C and D) Heat map (C) and box plot (D) of m^{6}A methylation-related prognostic lncRNAs expression in COAD tumors and adjacent normal tissues. (E) Differential expression of immune checkpoints in COAD and paracancerous normal tissue species. *p<0.05, **p<0.01, ***p<0.001.

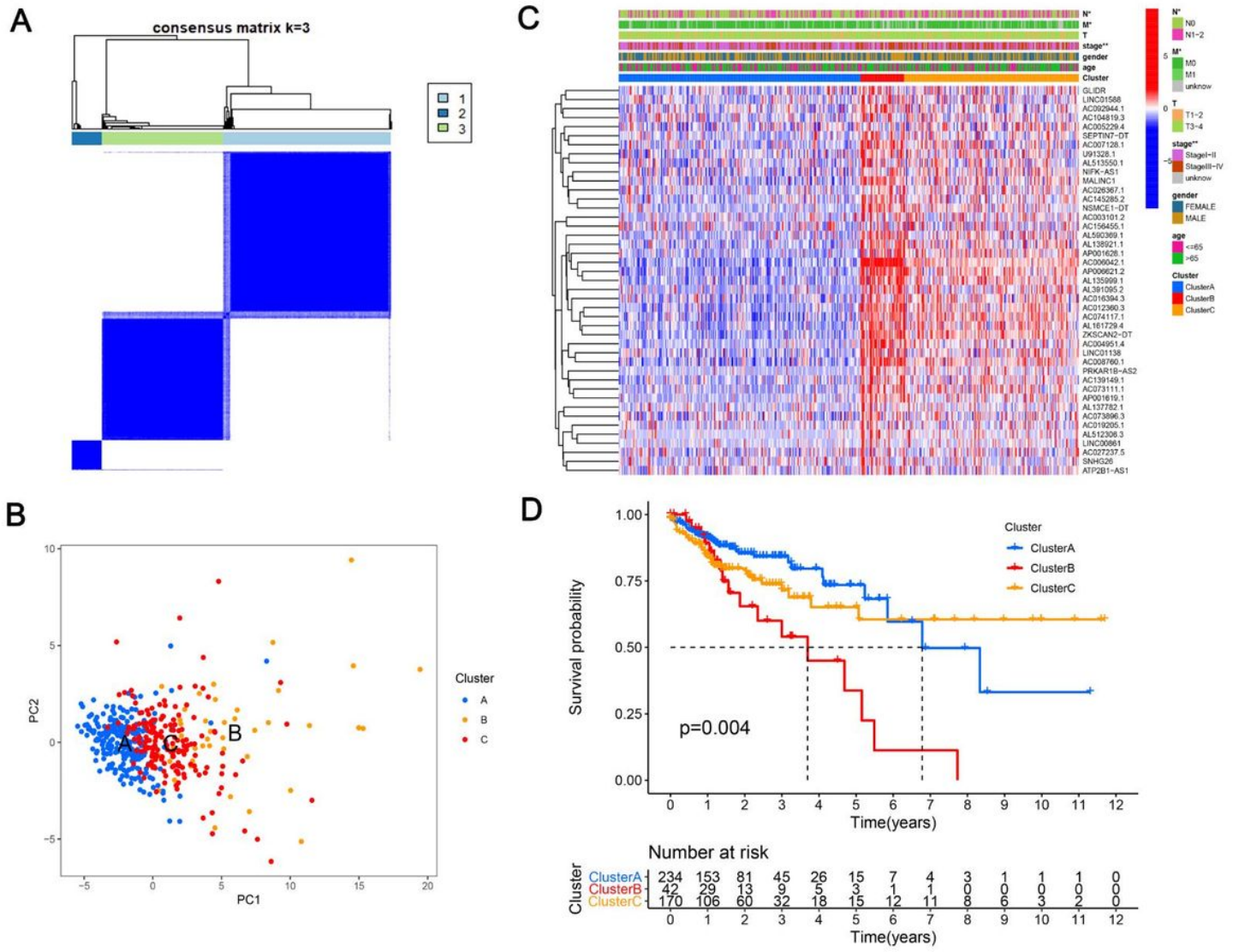

Figure 2

Different clinical attributes and survival rates of COAD subtypes in groups A, B, and C.

(A) Consensus clustering matrix with k=3. (B) PCA principal-form analysis. (C) Clinical correlation heatmap of the 3 clusters (clusters A, B, and C). (D) Kaplan-Meier curves for overall survival of patients with COAD in the 3 groups. *p<0.05 and **p<0.01, *** p<0.001.

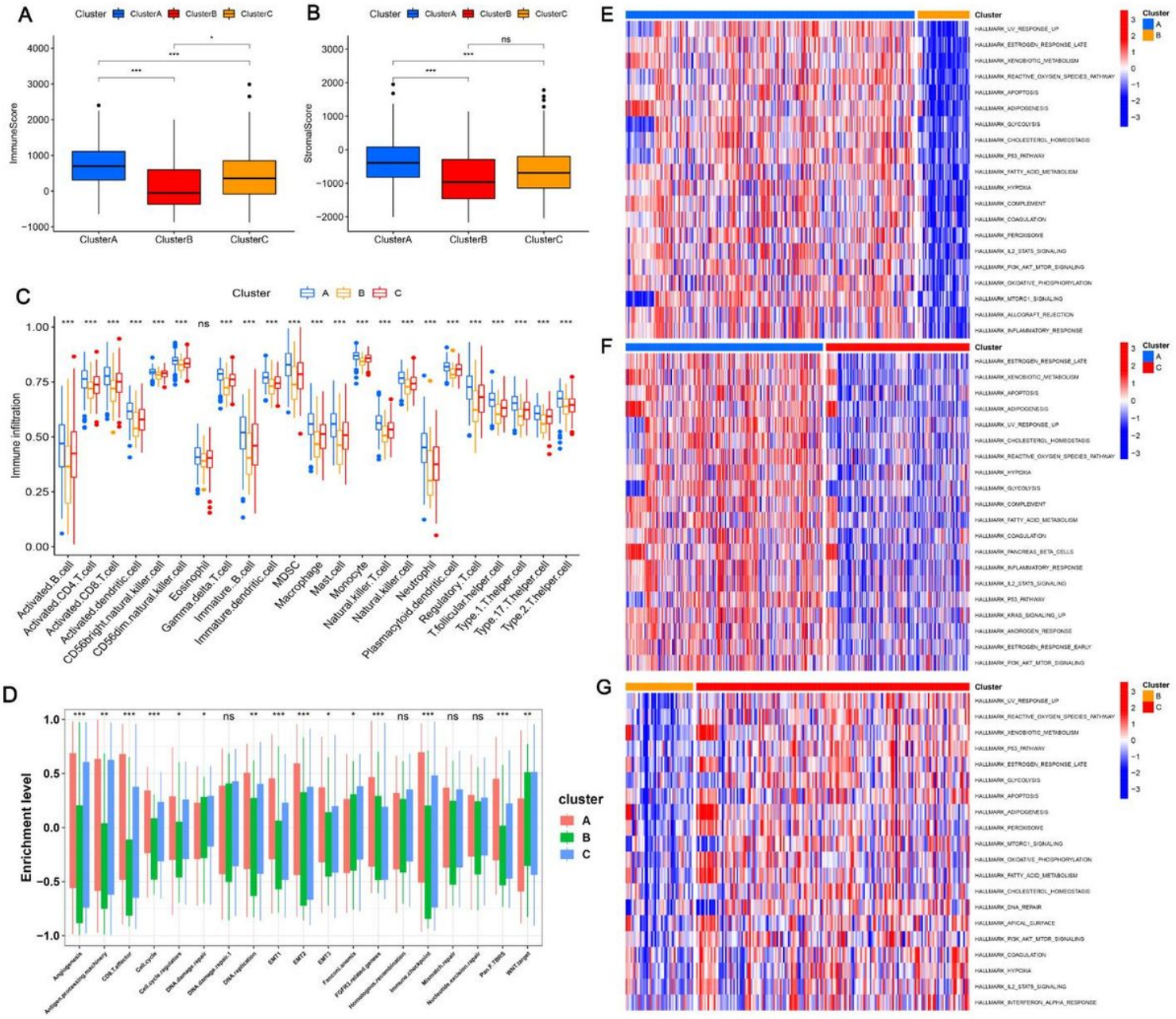

Figure 3

Differences in immune scores and immune cell infiltration between different subgroups.

(A, B) Immunoscore (A) and stromal score (B) of cluster A, B, and C subtypes. (C) Infiltration levels of 23 immune cell types in cluster subgroups. (D) Distinguish clusters A, B and C by different signatures (E-G) GSVA enrichment analysis showing the activation status of biological pathways under different m^{6}A modification patterns, (E)cluster A vs cluster B, (F) cluster A vs cluster C (G) cluster B vs cluster C. Heat maps were used to show these biological processes, with red representing activation pathways and blue representing inhibition pathways. the COAD cohort was used as sample annotation. *p<0.05 and **p<0.01, *** p<0.001.

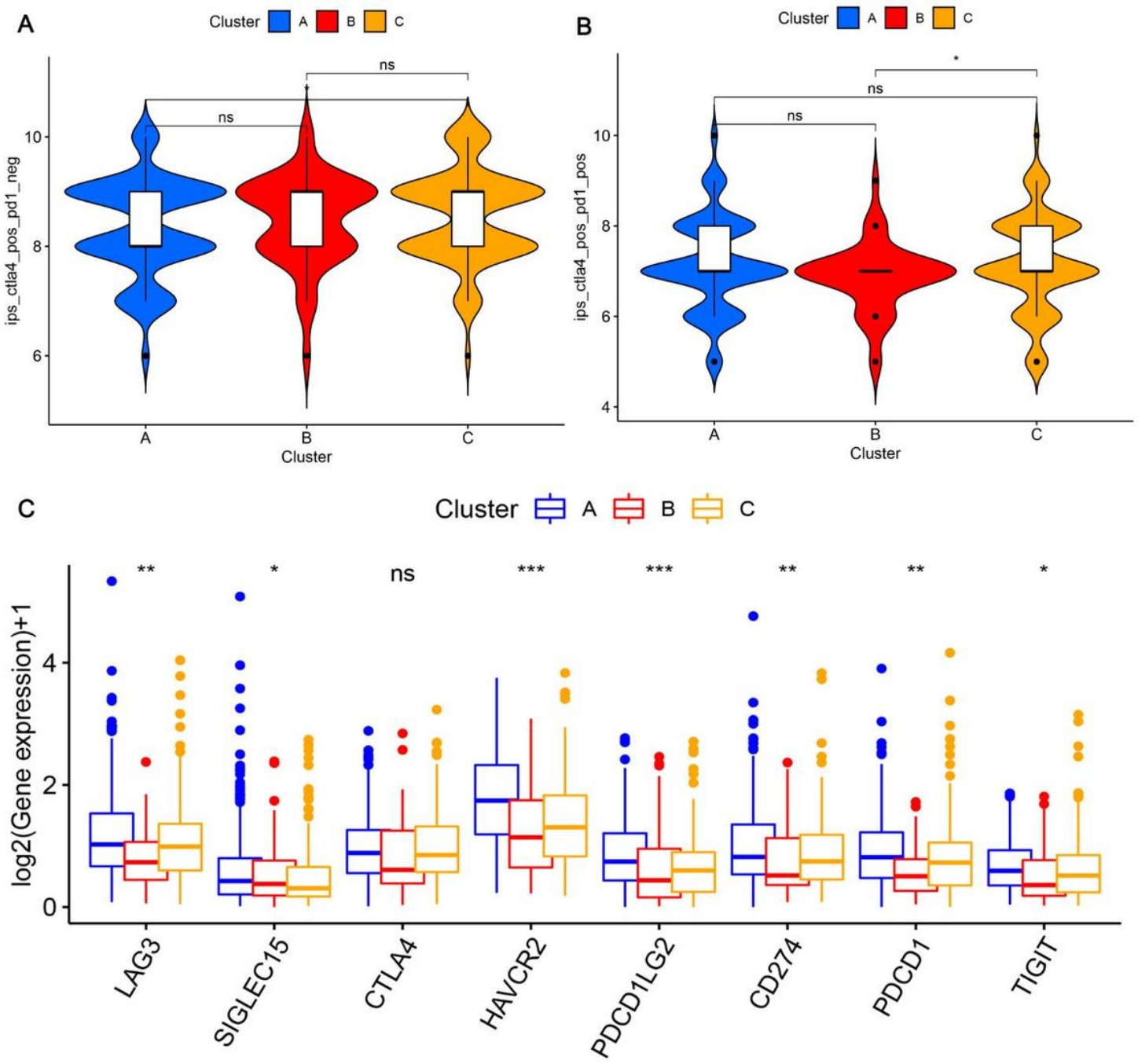

Figure 4

Cluster A, B, and C subtypes correlate with predictors of immunotherapy efficacy.

(A) IPS score of *CTLA4* alone effect for cluster A, B, and C subtypes. (B) IPS score of cluster A, B, and C subtypes in *CTLA4* and *PD1* combination effect. (C) Differential expression of immune checkpoints in cluster A, B and C. *p<0.05 and **p<0.01, *** p<0.001. *p<0.05 and **p<0.01, *** p<0.001.

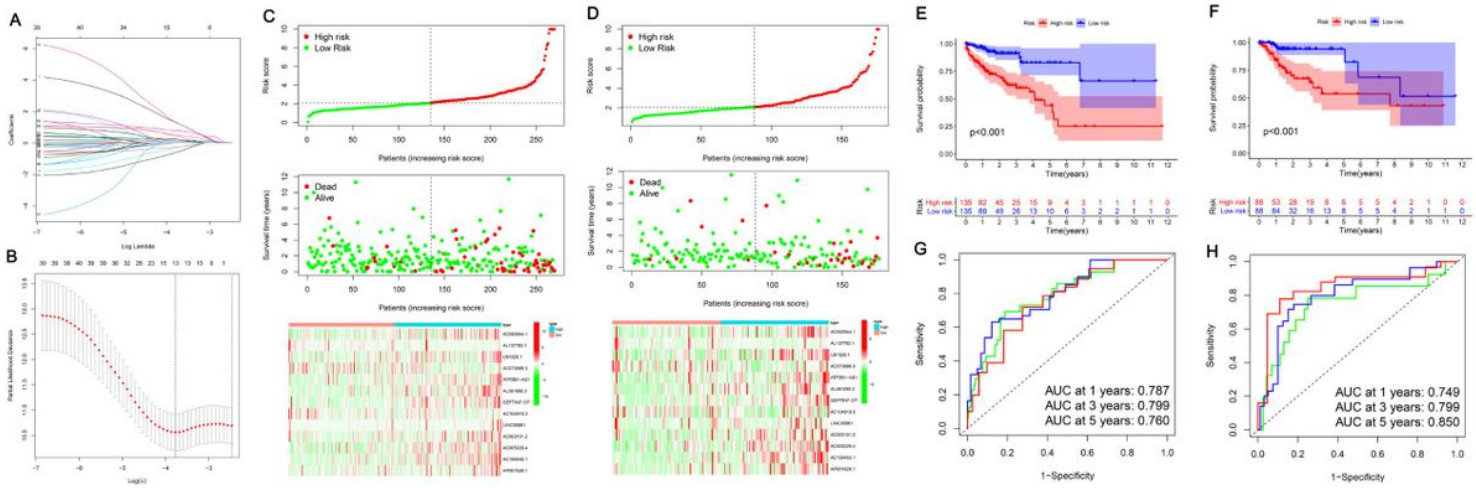

Figure 5

Construction and validation of m^{6}A methylation-related prognostic lncRNAs prediction signature.

(A and B) The least absolute1 shrinkage and selection operator (LASSO) regression was performed, calculating the minimum criteria. (C and D) Distribution of risk scores, OS status, and heat maps for 13 predictive m^{6}A-associated lncRNAs in the TCGA training cohort (C) and TCGA validation cohort (D). (E and F) Kaplan-Meier curves of OS in COAD patients according to risk scores in the TCGA training cohort (E) and validation cohort (F). (G and H) ROC curves for risk scores predicting 1-, 3-, and 5-year survival in the TCGA training cohort (G) and TCGA validation cohort (H).

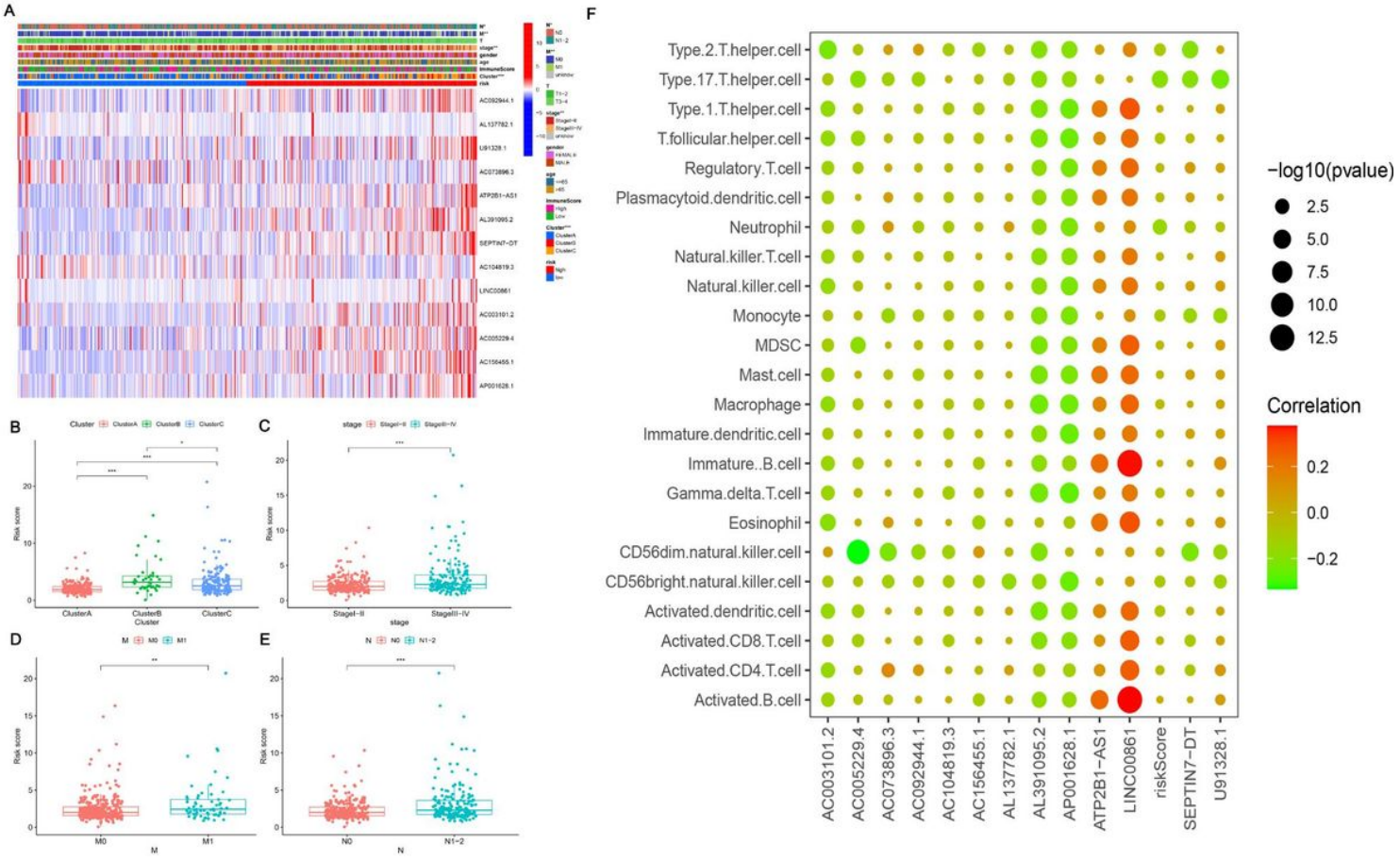

Figure 6

Prognostic risk scores correlated with immune score and TNM staging.

(A) Heatmap and clinicopathological features in high- and low-risk groups. (B-E) Distribution of risk scores stratified by cluster A, B, C, (B) TMN staging (C), presence of distant tumor metastases (D) and lymph node metastases (E), (F) Association of methylation-related prognostic lncRNAs predictors and risk scores with immune cell infiltration. *p<0.05, **p<0.01, ***p<0.001.

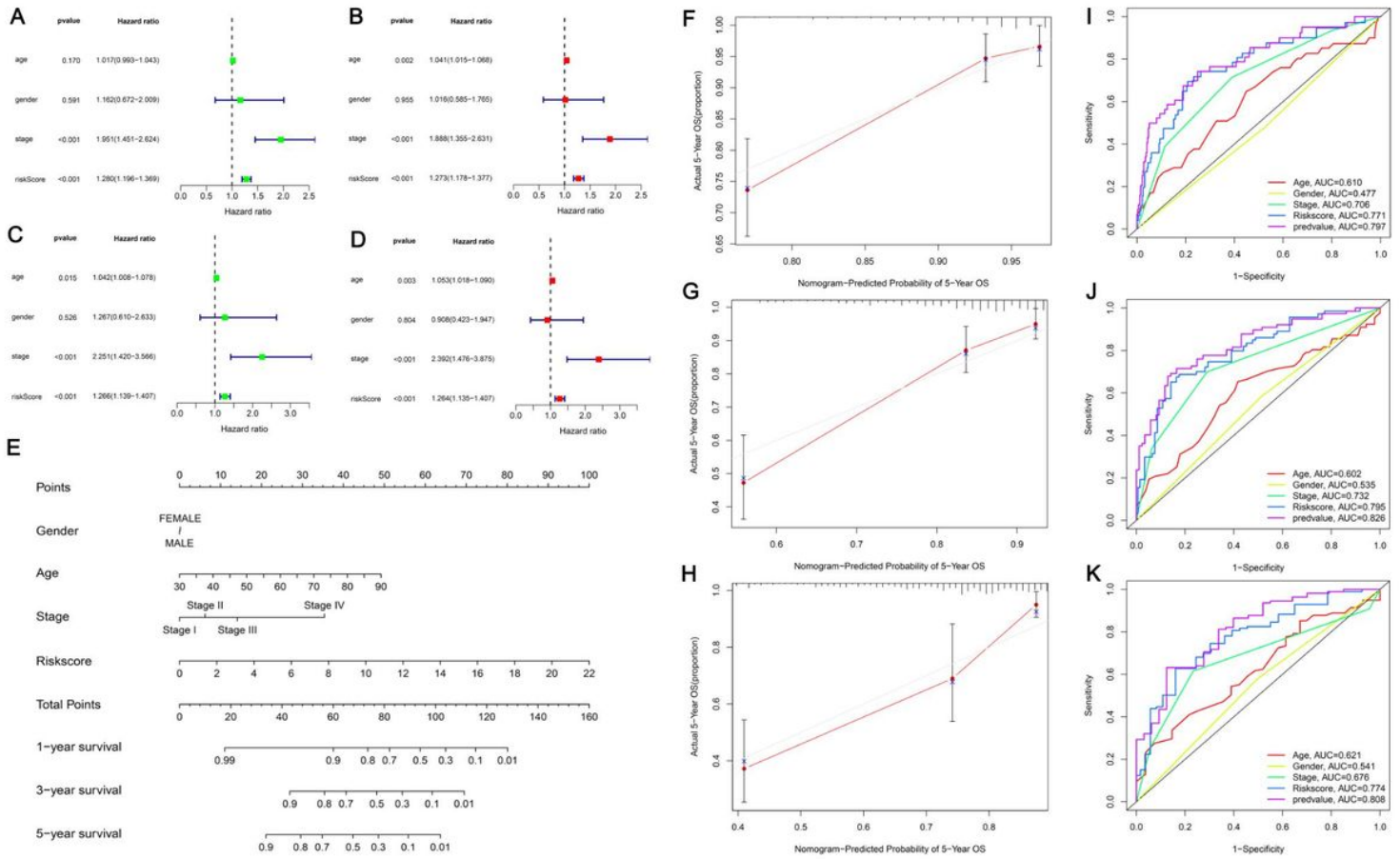

Figure 7

Construction and validation of Nomogram.

(A, B) Single-factor analysis (A) and multi-factor (B) analysis in the training cohort. (C, D) Single-factor (C) and multi-factor (D) analysis in the validation cohort. (E) Nomogram based on risk score, age, gender, and TNM staging. (F, G, H) Calibration curves for 1, 3, and 5-year OS (I, J, K) Nomograms for 1, 3, and 5 years compared with risk scores and AUC curves for different clinical characteristics.

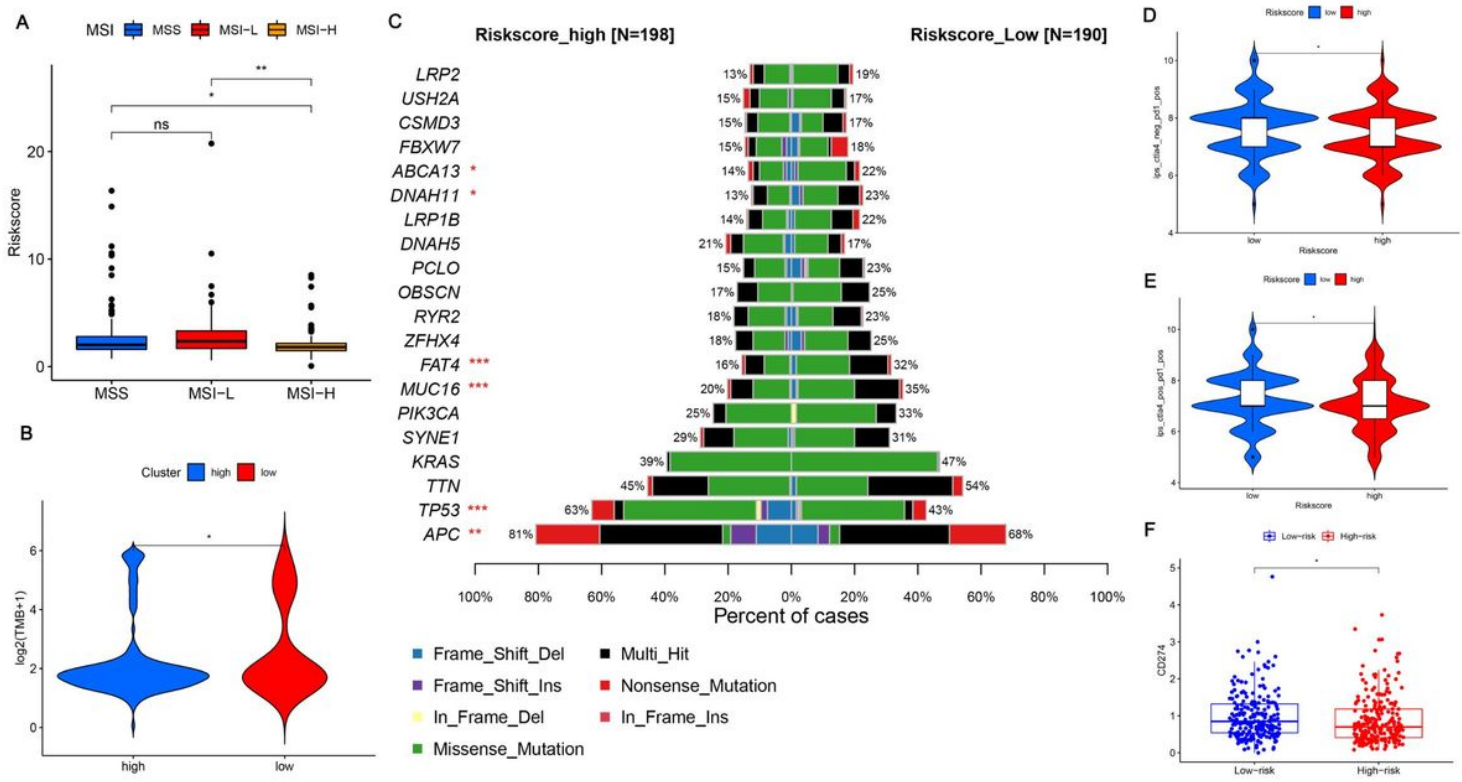

Figure 8

Relationship between risk score and microsatellite instability, tumor mutation load, and immune checkpoints.

(A) Microsatellite instability. (B) Tumor mutational burden. (C) Significantly mutated gene (SMG) analysis. (D, E) IPS scores for *PD1* alone (D) and *PD1* combined with *CTLA4* (E) in the high and low scoring groups. (F) Differences in *CD274* expression between the high- and low-risk groups *p<0.05 and **p<0.01, *** p<0.001.

Supplementary Files

This is a list of supplementary files associated with this preprint. Click to download.

- TableS1.docx